surfaces

MDPI

Article

A Comparative Study of Dip-Coating and Drop-Casting for Surface Modification of Kraft Paper with Silver Nanoparticles Toward Active Packaging

Naiara Milagres Augusto da Silva [1,2], Juliana Junqueira Pinelli [1], Cínthia Caetano Bonatto [1] and Luciano Paulino Silva [1,2,*]

[1] Laboratory of Nanobiotechnology (LNANO), Embrapa Genetic Resources and Biotechnology, Parque Estacao Biologica, Final W5 Norte, Brasília 70770-917, DF, Brazil; naiara.milagres@embrapa.br (N.M.A.d.S.); jujjpinelli@gmail.com (J.J.P.); cinthiabonatto@gmail.com (C.C.B.)

[2] Postgraduate Program in Nanoscience and Nanobiotechnology, University of Brasilia (UnB), Brasília 70910-900, DF, Brazil

* Correspondence: luciano.paulino@embrapa.br

Abstract

Kraft paper, commonly known as brown paper, has been widely used in the preservation of various food products and is increasingly explored in the development of active packaging materials with antimicrobial functionality by incorporating metal nanoparticles. This study aimed to comparatively investigate the surface modification of Kraft paper with silver nanoparticles (AgNPs) using dip-coating and drop-casting techniques. AgNPs were produced via green synthesis and incorporated onto the surface of Kraft paper samples. The modified samples were characterized using physicochemical techniques, including atomic force microscopy (AFM), Raman spectroscopy and light microscopy, as well as nanomechanical characterization via force spectroscopy. The antimicrobial activity of the modified papers was assessed using the disk diffusion method. The results demonstrated that the modification techniques resulted in distinct surface characteristics. Samples treated with the drop-casting method exhibited the highest AgNP surface loading; however, this was accompanied by pronounced surface heterogeneity and a tendency toward reduced load-bearing capacity. Overall, the findings indicate that the choice of deposition technique plays a key role in controlling nanoparticle distribution and surface properties. Within the limitations of the techniques evaluated, the incorporation of nanomaterials with potential antimicrobial activity into Kraft paper may offer opportunities for the development of active food packaging, although further optimization is required.

Keywords: thin films; silver nanoparticles; dip-coating; drop-casting; antimicrobial activity; kraft paper

Academic Editors: Liuhua Mu and Xiaoyan Li

Received: 9 December 2025
Revised: 17 February 2026
Accepted: 21 February 2026
Published: 24 February 2026

1. Introduction

Kraft paper, commonly known as brown paper, is a cellulose fiber-based material traditionally used in packaging applications due to its favorable mechanical properties, renewability, and cost-effectiveness. Its manufacturing process begins with debarked raw wood that is mechanically reduced to chips, which are subsequently screened to ensure suitable particle size for pulping [1]. The resulting cellulose pulp undergoes refining, a mechanical treatment that partially breaks the fibers and increases their specific surface area, enhancing fiber–fiber bonding [2]. Paper sheet formation occurs through the deposition

of an aqueous fiber suspension onto a forming screen, where the fibers interlace to form a porous, tissue-like network. Water removal is achieved by mechanical pressing followed by thermal drying using heated cylinders [3].

Due to its favorable mechanical properties, Kraft paper is widely used for the packaging of various food products, including dry, frozen, and fresh foods [4]. However, ensuring food safety and maintaining product quality throughout storage and distribution remain major challenges for the food industry. In this context, the development of active packaging materials with antimicrobial functionality has attracted increasing attention, as such systems can prevent microbial adhesion and proliferation, thereby extending shelf life and preserving food quality [5]. Current strategies to provide antimicrobial functionality to Kraft paper primarily rely on surface modification approaches rather than bulk modification of the cellulose matrix. These methods include surface coatings incorporating metallic nanoparticles, such as silver (AgNPs), zinc oxide (ZnO), and copper oxide (CuO), which are widely recognized for their broad-spectrum antimicrobial activity. In parallel, biopolymer-based coatings such as chitosan, carboxymethylcellulose, and other cellulose derivatives have been employed, either alone or as matrices, for immobilizing antimicrobial agents, aiming to enhance nanoparticle retention, reduce migration, and improve coating stability [6]. The antimicrobial effectiveness of these systems is strongly influenced by the coating technique, nanoparticle distribution, and the degree of interaction between the active agents and the cellulose substrate, emphasizing the importance of deposition strategy in the design of antimicrobial Kraft paper for food packaging applications.

Silver nanoparticles (AgNPs), in particular, have demonstrated high antimicrobial efficacy, relatively low production cost, and feasibility for large-scale processing [7]. However, the application of AgNPs in food-contact materials raises concerns regarding the potential migration of particles or metal ions into the food product and the associated implications for consumer safety. Current knowledge on migration behavior and exposure risks remains limited, therefore further studies are necessary to elucidate not only antimicrobial performance but also migration levels and evaluate their potential impact on consumer safety [8].

Surface modification of paper-based materials with AgNPs can be achieved through various deposition techniques, including dip-coating and drop-casting. Dip-coating involves the controlled immersion and withdrawal of a substrate from a nanoparticle-containing solution, typically resulting in relatively uniform thin films [9]. In contrast, drop-casting consists of the direct deposition of a defined solution volume onto the substrate surface, followed by solvent evaporation, which may lead to localized nanoparticle accumulation and a more heterogeneous coverage [10] (Figure 1). Although both techniques have been individually applied to functionalize cellulose-based materials, systematic comparative studies evaluating how these deposition methods affect nanoparticle distribution and the resulting mechanical and functional properties remain scarce. In particular, the relationship between deposition technique, surface morphology, and antimicrobial performance of AgNP-modified Kraft paper has not been clearly established. These techniques differ markedly in film uniformity, nanoparticle distribution, and operational practicality, therefore the intrinsic differences between dip-coating and drop-casting may lead to distinct nanoparticle distributions and surface architectures and influence the functional properties of the final material.

Therefore, the aim of this study was to comparatively investigate the surface modification of Kraft paper with silver nanoparticles (AgNPs) using dip-coating and drop-casting techniques, with a focus on elucidating how the deposition methods influence nanoparticle distribution, surface characteristics and antimicrobial activity. The findings aim to

provide insights into the selection of appropriate surface modification strategies for the development of safe and effective active packaging materials.

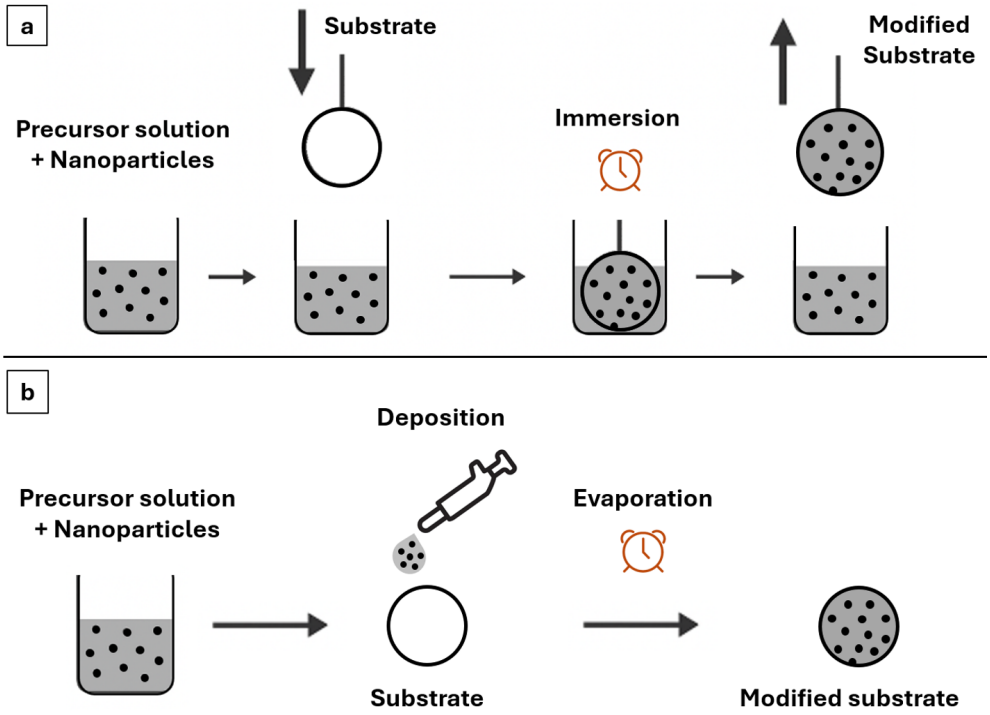

Figure 1. Schematic representation of thin-film coating techniques: (**a**) Dip-coating; (**b**) Drop-casting.

2. Materials and Methods

2.1. Materials

All solutions were prepared using ultrapure water and analytical-grade reagents. The materials used included silver nitrate ($AgNO_3$) (Plat-Lab, Guarulhos, Brazil); Kraft paper (Natural Kraft Paper, 80 g/m^2, Code PBM6030, 60 cm × 200 m); *Escherichia coli* (ATCC 8739, Manassas, VI, USA); LB (Luria–Bertani) broth (Lennox), Ref. L3022 (Sigma–Aldrich, St. Louis, MO, USA); bacteriological agar (Agar No. 1), Ref. LP0011B (Oxoid, UK); and a stabilized solution containing 10,000 U of penicillin and 10 mg/mL of streptomycin.

2.2. Synthesis and Characterization of Silver Nanoparticles (AgNPs)

Silver nanoparticles (AgNPs) were provided by the Nanobiotechnology Laboratory (LNANO), Ispra, Italy, at Embrapa Genetic Resources and Biotechnology (Cenargen). The nanoparticles were produced in an earlier work, through a green synthesis method, using an aqueous extract of *Caryocar brasiliense* (Pequi) leaves [11], with authorization for access to genetic patrimony (CGEN n. 02001.007580/2014-95). In that prior study, for the synthesis of AgNPs, 5 mL of the aqueous leaf extract of *C. brasiliense*, at a concentration of 100 mg/mL (plant material basis), were added to 495 mL of an aqueous silver nitrate ($AgNO_3$) solution (Plat-Lab, Guarulhos, Brazil) at a concentration of 1 mM, resulting in final concentrations of 1 mg/mL of plant extract and 1 mM of $AgNO_3$ in the reaction medium. The reaction was carried out in glass beakers, protected from light and the reaction mixture was maintained at 75 °C for 150 min. The formation of AgNPs was monitored by visual color change and UV–Vis absorption spectroscopy at 450 nm (Quimis, Sao Paulo, Brazil). In the previous study, the AgNPs were fully characterized in terms of their physicochemical and structural properties, after which the suspension was stored at 4 °C until further use.

In the present study, the AgNPs were not re-synthesized. Instead, the previously stored suspension was used for surface deposition onto Kraft paper. Prior to deposition,

the suspension was re-characterized by T dynamic light scattering (DLS) to determine the hydrodynamic diameter (HD) and polydispersity index (PdI). Zeta potential (ZP) was measured by electrophoretic mobility to confirm its colloidal stability [12]. All analyses were carried out using a ZetaSizer Nano (Malvern Instruments, Malvern, UK). The nanoparticle suspension was diluted 10-fold in ultrapure water and DLS measurements were performed at a scattering angle of 173°, using a 4 mW He-Ne laser with a wavelength of 633 nm. Three measurements were taken per sample at 25 °C under automatic mode. Data were analyzed using ZetaSizer software (version 8.02, Malvern Instruments, Malvern, UK) and results are reported as arithmetic mean and standard deviation.

2.3. Surface Modification of Kraft Paper

Kraft paper samples (Natural Kraft Paper, 80 g/m^2, Code PBM6030, 60 cm × 200 m) were cut into 7 mm diameter circles using a paper punch. For surface coating via the dip-coating technique, paper samples were manually immersed, using fine-tipped tweezers, in the aqueous AgNPs suspension at the concentration obtained from synthesis using a 1 mM $AgNO_3$ precursor. Each sample was immersed once and remained in the suspension for 5 s, after which it was slowly withdrawn at a constant, manually controlled speed and transferred to a glass Petri dish (100 mm × 15 mm), where they were placed onto a piece of fixed Parafilm. For the drop-casting technique, Kraft paper circles were placed directly onto fixed Parafilm within a Petri dish of the same dimensions. Subsequently, 60 µL of the aqueous AgNPs suspension was deposited onto each sample.

Control samples for each technique were prepared following identical procedures but using distilled water instead of the AgNPs suspension. All samples were then placed in a glass desiccator (250 mm × 250 mm) containing silica gel and allowed to dry for 48 h (Figure 2).

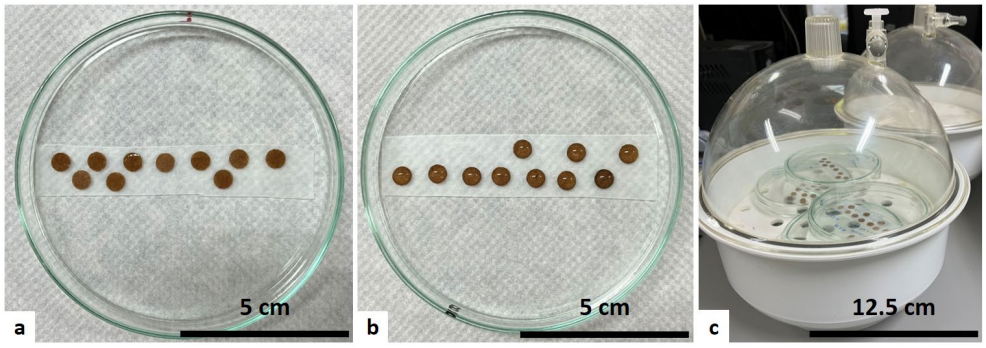

Figure 2. Kraft paper samples coated with AgNPs suspension: (**a**) modification by dip-coating; (**b**) modification by drop-casting; (**c**) drying of samples in a glass desiccator with silica gel.

2.4. Physicochemical Characterization

Physicochemical characterization of the samples was performed using atomic force microscopy (AFM) to obtain high-resolution topographic and phase images. Additionally, Raman spectroscopy, a technique based on inelastic light scattering characteristic of functional groups or chemical bonds, was employed to assess the chemical composition and structural features of the materials [13].

2.4.1. Atomic Force Microscopy (AFM)

Topographic (height) and phase (viscoelasticity) images were acquired using an atomic force microscope (SPM-9600 Shimadzu, Kyoto, Japan) operating in dynamic mode, with phase acquisition under constant force. A 125 µm rectangular cantilever was used, with a spring constant of 42 N/m and a resonance frequency of approximately 320 kHz, inte-

grated with a silicon pyramidal tip with a curvature radius of less than 10 nm. Scans were performed on two distinct regions (10 × 10 μm) of representative coated samples and its corresponding control, at room temperature (~22 °C) and used to qualitatively assess surface morphology and AgNPs distribution at the microscale. Images were processed using SPM-9600 software (version 3.03, Shimadzu, Kyoto, Japan), with automatic plane correction and X-axis leveling to enhance visualization and analysis, ensuring accurate representation of the topography relative to a corrected plane. The same software was used to calculate quantitative surface roughness parameters, specifically average roughness (Ra), which was used as a descriptive parameter to compare local surface features between samples.

2.4.2. Force Spectroscopy

Nanomechanical characterization of the samples was performed using force spectroscopy with an atomic force microscope (SPM-9600 Shimadzu, Kyoto, Japan) operating in contact mode. A 200 μm cantilever with a spring constant of 0.15 N/m and a resonance frequency of approximately 24 kHz was used, equipped with a silicon nitride pyramidal tip with a curvature radius of less than 20 nm.

To account for the intrinsic heterogeneity of Kraft paper, force–distance measurements were collected at multiple, spatially distinct locations across each sample surface. Ten force–distance curves were acquired at room temperature (~22 °C) for each treated sample and the corresponding controls. The curves were processed using SPIP-Scanning Probe Image Processor (version 5.1.11, Image Metrology, Hørsholm, Denmark), to extract quantitative data on local mechanical properties. Processing included automatic zero-point definition, baseline adjustment using the approach curve, and averaging of approach and retraction curves. Data were statistically analyzed using SISVAR software (version 5.8, Federal University of Lavras, Lavras, Brazil) with mean comparison performed using Tukey's test at a significance level of 0.05.

2.4.3. Light Microscopy

Images of the Kraft paper samples were obtained using a light microscope (Nikon, Japan) equipped with a digital camera (Digilab, Piracicaba, Brazil), and digitally recorded using Image View software, version 3.7. Image acquisition was performed at different regions of each sample to capture surface variability. The images were subsequently processed using the machine learning tool Teachable Machine (Google, Mountain View, CA, USA), which enables automated classification based on predefined patterns. The classification model was trained using 40 images acquired from multiple areas of representative samples of each treatment and the corresponding controls. An independent dataset of ten images per group, obtained from distinct surface regions, was subsequently used to evaluate the model's classification accuracy and prediction confidence.

2.4.4. Raman Spectroscopy

Raman spectra were acquired from representative coated samples and the corresponding control groups, using a confocal Raman microscope (Alpha 300 RA, WITec, Ulm, Germany) equipped with a diode laser module with a wavelength of 785 nm and a power of 400 mW. Spectra were collected with an integration time of 0.4 s and 100 accumulations. The resulting spectra were processed by applying baseline correction and smoothing to reduce spectral noise and facilitate qualitative interpretation.

2.5. Antimicrobial Activity

To evaluate the antimicrobial effect of AgNPs incorporation onto Kraft paper surfaces, in vitro antibacterial assays were conducted using the disk diffusion test. This method assesses the formation of inhibition zones, which reflect the diffusion and efficacy of an-

timicrobial compounds. The assay was designed to provide a comparative evaluation of antimicrobial performance between treatments under identical experimental conditions, rather than an absolute quantification of antimicrobial efficacy. In this study, the antimicrobial activity of the samples was evaluated against *Escherichia coli* (ATCC 8739), a Gram-negative bacillus of relevance to food safety, due to its high contamination potential in various food products [14].

The liquid culture medium used was LB (Luria–Bertani) Broth (Lennox), Ref: L3022 (Sigma-Aldrich, St. Louis, MO, USA), prepared according to the manufacturer's instructions. For solid medium preparation, bacteriological agar (Agar No. 1), Ref: LP0011B (Oxoid, UK), was added to the LB medium. Inoculum standardization was performed using a single-beam biophotometer (BioPhotometer model 6131, Eppendorf, Hamburg, Germany), applying the McFarland scale to reach an optical density (OD) of 0.5, corresponding to approximately 10^8 CFU/mL (colony-forming units per milliliter). The inoculum was subsequently diluted to a working concentration of 10^7 CFU/mL. Finally, 100 µL of the diluted inoculum was added to each Petri dish and evenly spread across the agar surface.

Kraft paper discs containing AgNPs, as well as control samples, were exposed to UV radiation for 20 min on a single surface, prior to antimicrobial testing. Given the porous and fibrous structure of Kraft paper, this single-sided UV exposure is insufficient to ensure complete sterilization of the material and may have contributed to the observed microbial contamination. The positive control was prepared by impregnating Kraft paper discs with 10 µL of a stabilized solution containing 10,000 U of penicillin and 10 mg/mL of streptomycin, used to verify bacterial susceptibility and to validate the performance of the disk diffusion assay. All treated and control samples were tested in triplicate. The discs were placed on the solid medium with the UV-exposed surface facing the agar surface. Plates were incubated at 37 °C and microbial growth and inhibition zone formation were monitored at 24, 48, and 72 h.

In addition to visual inspection, photographic records of the plates were acquired at each time point. The images were subsequently analyzed using Image J software (version 1.53m, National Institutes of Health, Bethesda, MD, USA) to determine the diameters of the inhibition zones in the diffusion assays.

3. Results and Discussion

3.1. Characterization of AgNPs

The AgNPs exhibited an average HD (Z-Average) of 78.72 ± 2.07 nm, a PdI of 0.435 ± 0.081, and a ZP of −13.4 ± 1.4 mV. These values represent the arithmetic mean and standard deviation of three independent measurements of the AgNPs suspension and indicate that the nanoparticles possess a relatively uniform size, a moderately narrow size distribution and a negative surface charge. These characteristics are consistent with stable colloidal systems and suggest the coexistence of small primary nanoparticles and larger aggregates or agglomerates in suspension. Similar findings have been reported for silver nanoparticles synthesized via green routes using plant extracts [15], where the AgNPs presented nanometric dimensions (73–104 nm), negative surface charge, and moderate polydispersity. The agreement between our findings and those reported for other green-synthesized AgNPs in the literature indicates that the green synthesis route used in the previous study to obtain the AgNPs evaluated here successfully promoted the formation of stable AgNPs within the expected nanometric range.

To gain a more accurate insight into the primary particle size, the size distribution by number was analyzed. While the Z-average is commonly used to describe the mean hydrodynamic size of near-monodisperse systems, for polydisperse samples, number-based distributions provide a more representative estimate of the dominant nanoparticle popula-

tion, as it minimizes the influence of larger particles present in smaller quantities [16]. The number-weighted average diameter of the nanoparticles was 27.92 ± 2.42 nm (Figure 3), corresponding to the predominant size of individual nanoparticles present in the suspension. The pronounced difference between the Z-average (~79 nm) and the number-weighted mean diameter (~28 nm) indicates that a small population of larger aggregates strongly influences the intensity-weighted DLS signal. This aggregation state is particularly relevant for interpreting surface deposition onto Kraft paper, as larger aggregates may preferentially adsorb at fiber junctions or surface irregularities, while smaller nanoparticles are more likely to penetrate the porous fiber network and contribute to a more homogeneous surface coverage [17]. Consequently, the coexistence of primary nanoparticles and aggregates may influence both coating morphology and antimicrobial performance, especially in diffusion-based assays. Therefore, combining Z-average data with number-based size distribution strengthens the interpretation of nanoparticle size heterogeneity and better reflects the actual population of smaller particles.

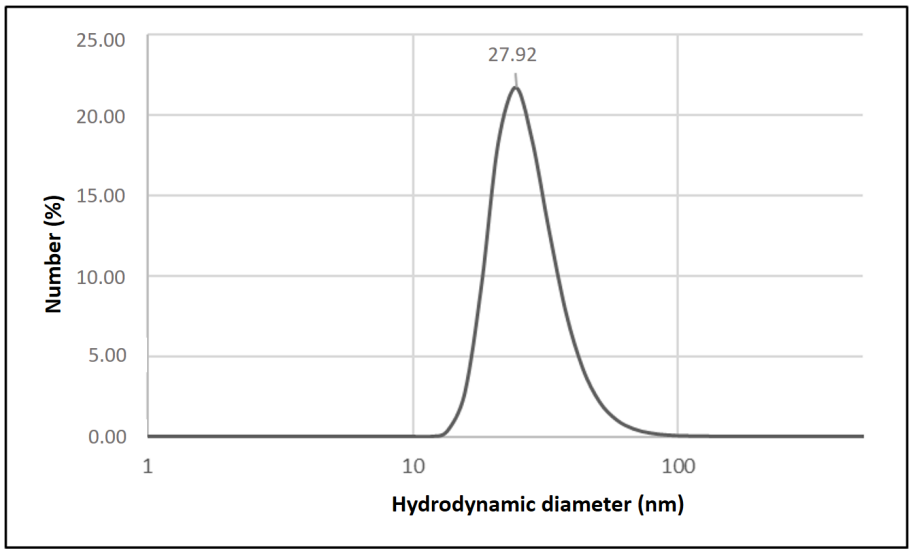

Figure 3. Number-weighted average diameter (nm) of AgNPs obtained by dynamic light scattering (DLS).

For the samples modified using the drop-casting technique, the equivalent amount of deposited silver was calculated based on the concentration of the AgNPs suspension, the molar mass of metallic silver and the volume applied to the Kraft paper (Equation (1)). From this value, the silver surface density was determined (Equation (2)), taking into account the exposed area of the paper discs used in the experiments. These parameters serve as useful indicators of the effective AgNPs loading on the paper surface. Previous studies on AgNP-impregnated cellulose substrates have demonstrated correlations between silver surface density and antimicrobial efficacy, as well as the AgNP stability and the potential risk of nanoparticle migration [18]. Thus, estimating both the mass and areal density of deposited AgNPs is relevant for predicting functional performance and potential food-contact safety considerations.

The molar mass of silver (Ag) is 107.8682 g/mol and the nanoparticle suspension used in this study was prepared from silver nitrate ($AgNO_3$) at a concentration of 1 mM. By applying 60 µL of this suspension to each Kraft paper sample, the estimated amount of deposited metallic silver was 6.47 µg per sample. Considering that the area of each circular paper disc was approximately 38.48 mm^2, the silver density per unit area was calculated as 0.168 $\mu g/mm^2$, according to the equations presented below. This value reflects a relatively high surface loading for cellulose substrates, reinforcing that drop-casting yields substantially greater nanoparticle retention than dip-coating.

With respect to existing regulations, the application of silver nanoparticles in food-contact materials is subject to strict evaluation due to concerns regarding nanoparticle migration, consumer exposure, and long-term safety. Current regulatory frameworks require case-by-case assessment of nanomaterials, emphasizing migration limits, material stability, and intended use conditions. In this context, the present study does not aim to establish regulatory compliance but rather provides mechanistic insights relevant to regulatory assessment. From a food-contact safety perspective, the migration of silver nanoparticles from packaging materials into food represents an important concern, as the uncontrolled release of silver ions (Ag^+) may pose risks to consumer health. Accordingly, regulatory agencies such as the European Food Safety Authority (EFSA) and the United States Food and Drug Administration (FDA) have established guidelines for the safety assessment of silver-containing materials intended for food contact. According to EFSA, the concentration of Ag^+ ions should not exceed 0.05 mg/L in water and 0.05 mg/kg in food [19]. In this context, the calculated surface silver density (0.168 μg/mm^2), corresponding to a total of 6.47 μg of silver per sample, can be interpreted as a conservative scenario when considering potential ionic migration, providing a relevant reference for future studies focused on Ag^+ migration assessment and regulatory compliance.

$$mAg = C \times M \times V \quad (1)$$

where

mAg: mass of deposited silver (μg)
C: concentration of $AgNO_3$ solution (mmol/L)
M: molar mass of silver (g/mol)
V: deposited volume (μL)

$$\rho Ag = mAg/A \quad (2)$$

where

ρAg: silver density per unit area
mAg: mass of deposited silver (μg)
A: surface area (mm^2)

3.2. Surface Modification of Kraft Paper

The modification techniques evaluated in this study differ fundamentally in the way the active compound is applied to the substrate surface. The dip-coating method requires immersing the substrate in a solution containing the compound of interest. The thickness and uniformity of the resulting coating are influenced by the withdrawal speed, the rheological properties of the suspension, and physical phenomena such as solvent evaporation, capillarity, and viscous drag. This technique offers advantages such as rapid thin-film formation, high efficiency in coating the entire surface, and the possibility of simultaneously coating both sides of the substrate [20]. However, a major limitation of this method is the difficulty in achieving homogeneous films with uniform thickness over the entire surface. This variability is particularly relevant for fibrous materials such as Kraft paper, whose porous and heterogeneous morphology strongly influences liquid uptake and retention during immersion.

In contrast, the drop-casting method consists of the controlled deposition of small volumes of the solution onto the substrate, followed by solvent evaporation. While this approach allows precise control over the applied volume, the final coating thickness may be highly heterogeneous due to particle redistribution during drying, commonly referred to as the "coffee-ring effect", which can result in localized nanoparticle accumulation and uneven surface coverage. Despite this limitation, drop-casting offers advantages such as operational simplicity, minimal solution waste, and rapid sample preparation [20]. For substrates with

low initial wettability, such as Kraft paper, drop-casting may also enhance nanoparticle retention by confining the suspension to the surface during solvent evaporation.

3.3. Atomic Force Microscopy

Surface characterization of the samples by AFM, operating in dynamic mode with phase acquisition, enabled the acquisition of high-resolution three-dimensional topographic images, revealing nanometric features such as roughness, undulations and detailed surface structures. Additionally, the phase images obtained (related to viscoelasticity) provided information about the local nanomechanical properties of the analyzed surfaces.

The topographic images (Figures 4–6) revealed elongated and entangled structures in all evaluated Kraft paper samples, consistent with the morphology of cellulose fibers comprising the material. During image acquisition, differences in surface morphology between the coated samples were observed. For samples treated by drop-casting, AFM imaging was partially limited by the vertical displacement range of the scanner (Z = 7 µm), resulting in intermittent loss of tip–sample contact during scanning. This behavior is indicative of pronounced surface roughness and agglomeration, likely formed during solvent evaporation and nanoparticle redistribution during the drop-casting process, which exceeded the vertical measurement capability of the instrument under the selected imaging conditions.

In all experimental and control groups, phase images evidenced regions with viscoelastic heterogeneity on the paper surface (Figures 4–6). This behavior is expected given the polymeric nature of cellulose fibers, whose molecular structure confers a mixed mechanical response, combining viscous properties typical of liquids with elastic characteristics akin to Hookean solids. This behavior, termed viscoelasticity, constitutes one of the most relevant intrinsic properties of polymers, directly influencing their functional performance in diverse applications [21]. These phase-contrast variations further confirm the complex microfibrillar arrangement characteristic of lignocellulosic substrates.

In the topography and phase images of the sample coated by drop-casting, structures suggestive of nanoparticles adhered to the surface of the Kraft paper were observed (Figure 6a,b), which were not identified in the control sample of this treatment (Figure 6c,d) nor in the other samples analyzed (Figures 4 and 5). The differences in the application technique of the active compound onto the surface to be modified, as previously noted, influence the adhesion capacity of the nanoparticles to the Kraft paper surface. It was indeed expected that the samples treated by drop-casting would present a greater number of nanoparticles, since the volume of suspension deposited onto the Kraft paper was substantially higher than the volume retained during dip-coating technique. Therefore, the increased nanoparticle presence in drop-cast samples likely enhanced their detectability in AFM analysis and contributed to the higher frequency of probe retraction events caused by surface protrusions.

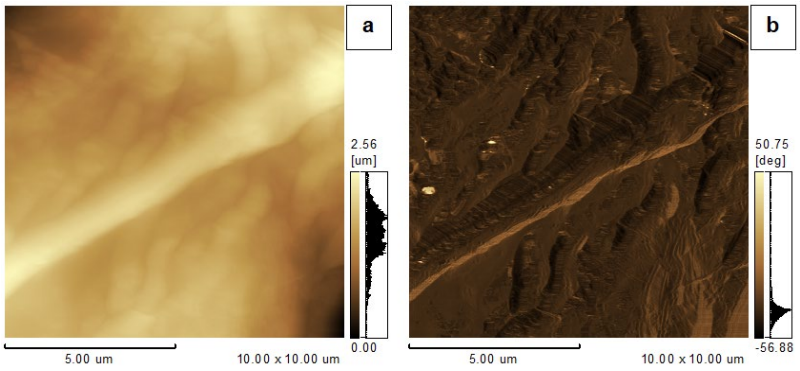

Figure 4. AFM images of the unmodified Kraft paper sample. (**a**) Three-dimensional topography image revealing surface morphology and organization of cellulose fibers; (**b**) Phase image showing local variations in the viscoelastic properties of the surface.

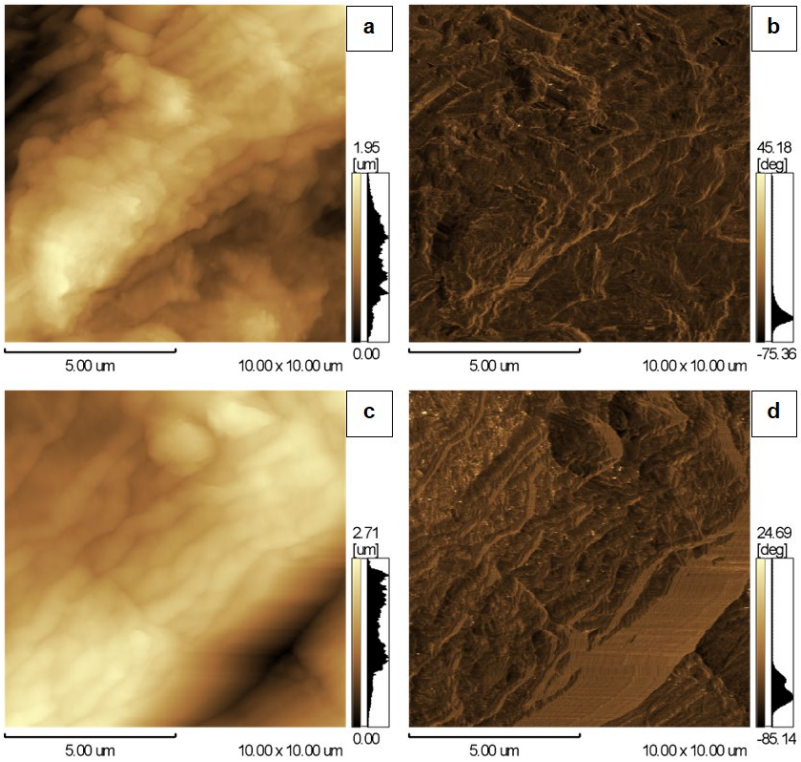

Figure 5. AFM images of Kraft paper samples coated with AgNPs suspension. Topography images are shown on the left; phase images are shown on the right. (**a**,**b**) Samples modified by dip-coating; (**c**,**d**) Control samples (unmodified).

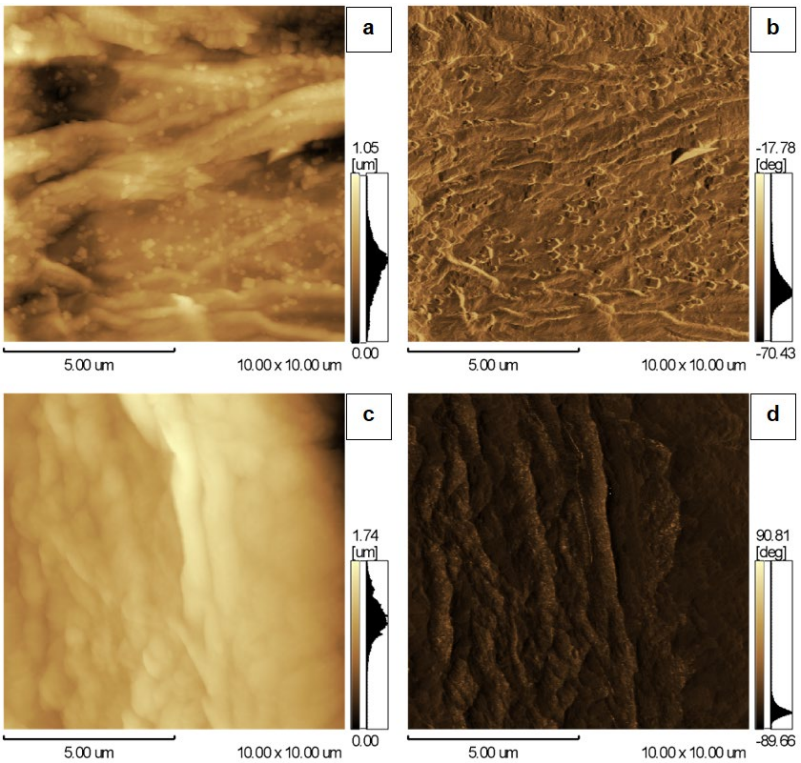

Figure 6. AFM images of Kraft paper samples coated with AgNPs suspension. Topography images are shown on the left; phase images are shown on the right. (**a**,**b**) Samples modified by drop-casting; (**c**,**d**) Control samples (unmodified).

Surface roughness parameters were calculated from AFM topographic images. The average roughness (Ra), expressed as numerical values, is presented in Table 1 solely as a qualitative indicator of relative surface roughness. All Kraft paper samples exhibited high Ra values, reflecting the intrinsically rough and heterogeneous nature of the material. Samples coated with AgNPs showed a consistent trend toward lower Ra values for both dip-coating and drop-casting methods, when compared to their respective controls (Table 1). This behavior suggests partial filling of surface depressions by nanoparticles or local smoothing of microfibrillar structures induced by nanoparticle deposition.

Table 1. Average roughness (Ra) values of Kraft paper samples evaluated by atomic force microscopy.

Sample	Unmodified Kraft Paper	Dip-Coating Control	Dip-Coating with AgNPs *	Drop-Casting Control	Drop-Casting with AgNPs *
Average roughness (Ra) (nm)	313.088	511.336	348.357	171.672	145.820

* Values correspond to the average Ra obtained from two different regions of a single sample.

3.4. Raman Spectroscopy

In the present study, the obtained Raman spectra did not exhibit visible characteristic peaks, and no differences were observed between the spectra of samples from the different treatments or the control groups (Figure 7).

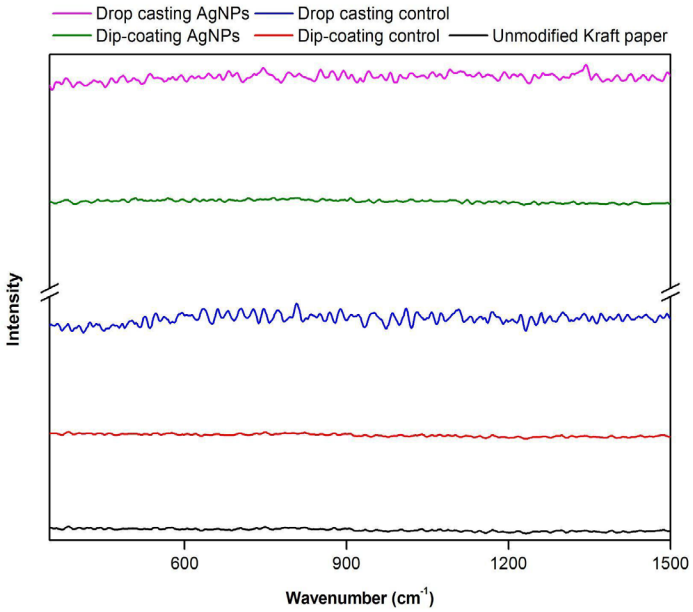

Figure 7. Representative Raman spectra obtained for Kraft paper samples.

The absence of visible peaks in the Raman spectra of the Kraft paper samples is a phenomenon previously reported in the literature [22,23] and can be attributed to the composition and physicochemical properties of Kraft paper. The presence of lignin and cellulose-derived compounds may interfere with spectroscopic analysis due to fluorescence emission, which is characteristic of lignocellulosic materials. Additionally, the vibrational modes of cellulose fibers often exhibit very low intensities, making their detection difficult against the spectral noise [23]. As a result, fluorescence can mask weaker Raman signals, leading to flattened spectra or spectra without noticeable peaks [22]. Thus, the flat or featureless spectra observed here align with known limitations of Raman analysis for lignocellulosic substrates, especially under high-fluorescence excitation conditions.

3.5. Light Microscopy

Images obtained by light microscopy revealed elongated and mesh-like structures on the surface of all Kraft paper samples, consistent with the findings obtained by AFM. These structures correspond to the cellulose fibers forming the material (Figure 8). A clearer visual distinction between fiber bundles and finer microfibrillar regions was also observed after revision of the images.

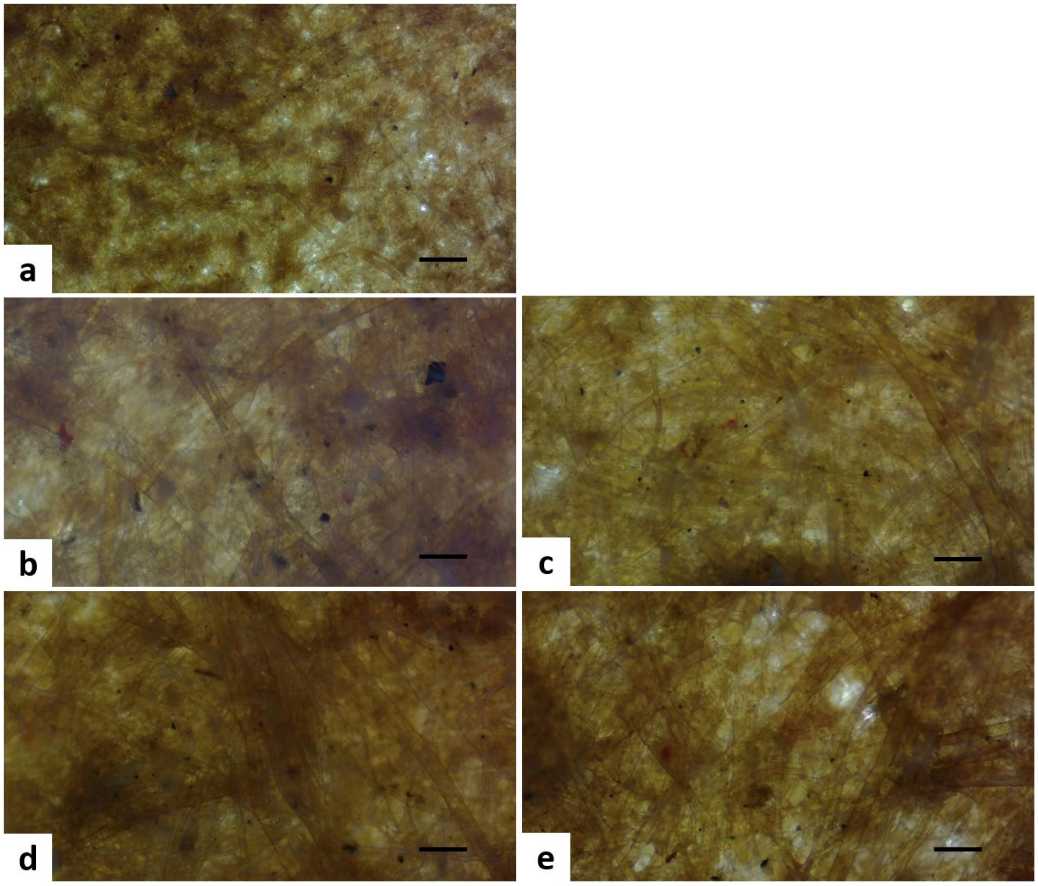

Figure 8. Representative images of Kraft paper samples obtained by optical microscopy at 10× magnification. (**a**) Unmodified Kraft paper; (**b**,**d**) Control samples; (**c**) Sample coated with AgNPs suspension by dip-coating; (**e**) Sample coated with AgNPs suspension by drop-casting. The scale bar corresponds to 80 µm.

The confidence percentages obtained from the classification of optical microscopy images using the Teachable Machine tool were used as a complementary and exploratory analysis to support surface morphology observations (Table 2). This approach was not intended to provide quantitative surface descriptors, but rather to evaluate whether morphological differences induced by the coating techniques could be qualitatively distinguished using automated image recognition. Unmodified Kraft paper samples exhibited the highest classification confidence, while samples treated by the drop-casting technique showed the lowest confidence levels. This trend is consistent with the higher surface heterogeneity observed for drop-cast samples by AFM analysis. The analysis of optical microscopy images using this machine learning tool further confirmed that the applied coating techniques induced distinct changes in the surface morphology of the samples. Specifically, drop-cast samples displayed greater irregularity in surface features, which likely reduced the model's ability to discriminate them from other classes.

Table 2. Mean and standard deviation values of confidence percentage for the correct classification of Kraft paper samples by the Teachable Machine tool.

Sample	Unmodified Kraft Paper	Dip-Coating Control	Dip-Coating with AgNPs	Drop-Casting Control	Drop-Casting with AgNPs
Confidence percentage (%)	99.60 ± 0.97	73.20 ± 28.39	79.50 ± 33.75	50.17 ± 41.39	32.80 ± 34.79

The high classification confidence and low variability observed for unmodified Kraft paper samples indicate that the model reliably identified surfaces with uniform and characteristic morphological features. For samples treated by dip-coating, the model maintained moderate classification performance, although with greater variability in confidence values, reflecting partial surface modification and intermediate morphological uniformity. Conversely, samples modified by drop-casting exhibited the lowest accuracy rates and the highest dispersion, suggesting increased surface heterogeneity that limited pattern recognition by the model. Rather than indicating model inadequacy, this behavior qualitatively supports the presence of non-uniform surface features resulting from nanoparticle redistribution and drying effects inherent to the drop-casting process.

To further visualize classification behavior, a confusion matrix was generated (Table 3), serving as an auxiliary tool to illustrate trends in correct and incorrect classifications. In this dataset, the "Sample" column represents the true class and the "Output" row indicates the categories assigned by the model. The percentage values express the proportion of times each class was assigned by the model, allowing identification of patterns of correct and incorrect classifications among the groups.

Table 3. Proportion of classifications assigned by the Teachable Machine tool to Kraft paper samples based on light microscopy images.

Sample \ Output	Unmodified Kraft Paper	Dip-Coating Control	Dip-Coating with AgNPs	Drop-Casting Control	Drop-Casting with AgNPs
Unmodified Kraft paper	100	0	0	0	0
Dip-coating Control	0	85	15	0	0
Dip-coating with AgNPs	0	0	80	0	20
Drop-casting Control	0	50	20	30	0
Drop-casting with AgNPs	0	0	30	30	40

Grayscale intensity is proportional to the percentage of images assigned to each class; darker cells indicate higher classification proportions.

The model correctly classified all unmodified Kraft paper samples, reinforcing their morphological distinctiveness and demonstrating excellent identification capability for this class. The greatest classification difficulties occurred for drop-cast samples, both control and AgNPs-treated groups, which exhibited lower accuracy (30% and 40%, respectively) and frequent misclassification with other classes. This overlap highlights the morphological variability introduced by the drop-casting process, which reduces the consistency of surface features available for automated discrimination. Overall, the machine learning-based analysis is presented as supportive qualitative evidence that aligns with AFM observations, reinforcing the conclusion that drop-casting produces surfaces with greater heterogeneity

than dip-coating. Further improvements in classification accuracy will likely require expanding the training dataset, especially for groups with high structural variability.

3.6. Force Spectroscopy

Force spectroscopy characterization yielded force-distance curves with highly variable profiles across the experimental groups and controls (Figure 9). This variability reflects both the intrinsic morphological and mechanical heterogeneity of cellulose fibers and the distinct nanoparticle distribution patterns resulting from each coating technique.

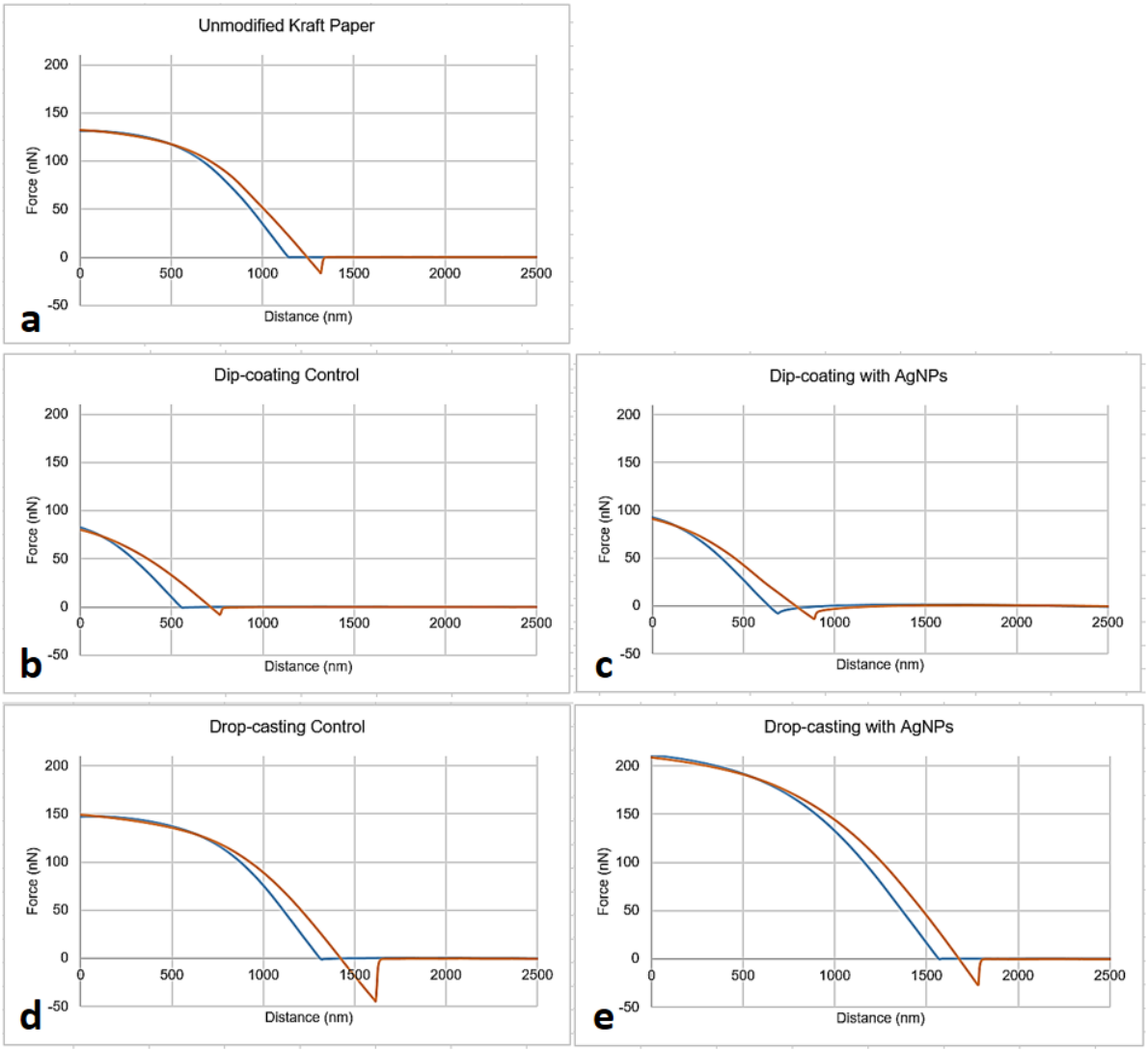

Figure 9. Force-distance curves obtained by force spectroscopy on Kraft paper samples. (**a**) Unmodified Kraft paper; (**b**,**d**) Control samples; (**c**) Sample coated with AgNPs suspension by dip-coating; (**e**) Sample coated with AgNPs suspension by drop-casting. In each plot, the blue line represents the approach curve (loading/indentation), while the orange line represents the retraction curve (unloading).

Based on the analysis of the force-distance curves, quantitative parameters associated with local nanomechanical properties of the samples were extracted, including maximum load, adhesion (pull-off) force, Young's modulus, and dissipated energy, with mean values and standard deviations summarized in Table 4.

Table 4. Mean and standard deviation values of nanomechanical properties of Kraft paper samples obtained by force spectroscopy.

	Maximum Load (nN)	Adhesion Force (nN)	Young's Modulus (Pa)	Dissipated Energy (J)
Unmodified Kraft paper	130.69 ± 25.042^{b}	30.74 ± 25.153^{a}	$2.87 \times 10^{6} \pm 1.33 \times 10^{6\,a}$	$1.06 \times 10^{-14} \pm 5.11 \times 10^{-15\,a}$
Dip-coating Control	84.17 ± 7.1735^{a}	24.82 ± 16.651^{a}	$2.80 \times 10^{7} \pm 7.90 \times 10^{6\,b}$	$7.12 \times 10^{-15} \pm 1.4 \times 10^{-15\,a}$
Dip-coating with AgNPs	91.91 ± 9.778^{a}	20.93 ± 7.9952^{a}	$2.85 \times 10^{7} \pm 7.74 \times 10^{6\,b}$	$8.31 \times 10^{-15} \pm 1.63 \times 10^{-15\,a}$
Drop-casting Control	138.09 ± 11.635^{b}	35.36 ± 20.1^{b}	$2.56 \times 10^{6} \pm 1.50 \times 10^{6\,a}$	$7.38 \times 10^{-15} \pm 3.12 \times 10^{-15\,a}$
Drop-casting with AgNPs	113.62 ± 57.734^{ab}	30.52 ± 21.66^{a}	$1.03 \times 10^{7} \pm 8.10 \times 10^{6\,a}$	$1.09 \times 10^{-14} \pm 7.4 \times 10^{-15\,a}$

Mean values within a column followed by the same lowercase letter are not significantly different according to Tukey's test ($p < 0.05$).

The maximum load represents the highest force, in Newtons (N), that the material can withstand before failure and is a key parameter in strength testing. The adhesion force, measured during probe retraction, reflects the interaction forces between the surface and the AFM tip, which are particularly relevant for understanding nanoscale interactions, especially in surface coating studies. Stiffness, also referred to as the elastic modulus or Young's modulus, describes the material's resistance to elastic deformation and is expressed in Pascal (Pa), the standard unit of pressure and stress. Dissipated energy corresponds to the total amount of energy absorbed or lost during the force-distance cycle. This parameter is calculated as the difference between the areas under the approach and retraction curves, representing energy that is not recovered during probe–sample interaction. Such energy dissipation may be associated with friction, irreversible deformation, or viscoelastic relaxation processes, which are relevant in the analysis of polymeric and fibrous materials exhibiting viscoelastic behavior [24].

The numerical reduction in the maximum load for drop-casting samples with AgNPs (113.62 nN), suggests a tendency toward reduced load-bearing capacity, indicating that the incorporated nanoparticles may introduce structural defects or act as stress concentrators, thereby potentially compromising the mechanical strength of the paper matrix [25]. This reduced load-bearing capacity may be associated with nanoparticle-induced surface discontinuities or weakening of fiber–fiber bonding interactions. This group also exhibited higher data dispersion, as reflected by the large standard deviation (57.73 nN), which is likely attributable to non-uniform dispersion and aggregation of the nanoparticles inherent to the drop-casting process. Although a numerical decrease in adhesion force was observed for drop-casting samples with AgNPs relative to their control, this difference was likely due to the high variability associated with surface heterogeneity and local nanoparticle aggregation [25].

Conversely, samples treated by dip-coating exhibited higher stiffness, indicating greater resistance to deformation. This behavior suggests that nanoparticle deposition via a thin, immersion-based coating may reinforce or rigidify the cellulose fiber network, possibly due to more uniform nanoparticle–fiber interactions. In contrast, the lower Young's modulus values observed for the other groups indicate that these materials deform more readily under applied force. Regarding the dissipated energy parameter, the measured values were low and did not differ statistically among the experimental groups. These results suggest that the dominant viscoelastic energy dissipation mechanisms were not systematically altered by the coating techniques or by AgNP incorporation, despite the observed differences in surface adhesion and stiffness.

Previous studies have demonstrated that the incorporation of silver nanoparticles into cellulose-based coatings can significantly enhance mechanical performance when nanoparticles are effectively immobilized within a polymeric or nanocellulosic matrix. For instance, carboxymethyl cellulose/cellulose nanocrystals/silver nanoparticles-coated paper exhibited increased tensile strength, improved barrier properties, and enhanced antibacterial activity with increasing nanoparticle content, effects attributed to the reinforcing role of cellulose nanocrystals and their strong immobilization of AgNPs [26]. In contrast, the more modest or inconsistent mechanical changes observed in the present study likely reflect differences in coating architecture and nanoparticle anchoring, as AgNPs were physically deposited onto the Kraft paper surface rather than embedded within a structured polymer–nanocellulose network. These comparisons highlight that mechanical reinforcement of paper substrates by AgNPs is highly dependent on the presence of binding matrices that promote uniform dispersion and effective load transfer.

Barrier properties of Kraft paper against oxygen, air, and water vapor can also be modified by the incorporation of metallic nanoparticles, including AgNP, by partially filling surface pores, altering fiber packing, and creating more tortuous diffusion pathways for gases and moisture. In cellulose-based systems, improved barrier performance has been reported when nanoparticles are uniformly immobilized within polymeric or nanocellulose-based coatings, whereas heterogeneous deposition or surface agglomeration may lead to limited or inconsistent barrier enhancement [27]. As barrier properties were not directly measured in the present study, their evaluation remains an important focus for future work aimed at correlating AgNP distribution, coating method, and multifunctional packaging performance.

3.7. Antibacterial Activity

The antimicrobial activity was evaluated using the disk diffusion test, a physical method based on the exposure of microorganisms to bioactive substances on solid culture media. In this method, the formation and diameter of the inhibition zone are related to the concentration of the tested substance and its antimicrobial efficacy [28]. However, in the present study, this assay was used as a qualitative screening tool to explore the potential antimicrobial behavior of AgNP-modified Kraft paper.

The inhibitory effect of the samples modified with AgNPs was monitored at 24, 48, and 72 h through visual assessment of bacterial growth and inhibition zone development. In the plates containing control group samples (unmodified Kraft paper and Kraft paper treated only with distilled water by dip-coating and drop-casting), microbial contamination was observed at all-time points (24, 48, and 72 h), with the presence of filamentous structures suggestive of fungal growth (Figure 10a–c). This widespread contamination indicates that Kraft paper does not provide inherent antimicrobial protection and highlights the susceptibility of porous, cellulose-based substrates to environmental contaminants.

Samples treated with AgNPs by the drop-casting technique exhibited inhibition zones at 24 and 48 h, indicating a transient inhibitory effect. However, microbial contamination was observed in these samples after 72 h, and the inhibition zones were no longer clearly distinguishable. This temporal loss of inhibition may be due to limited nanoparticle diffusion, depletion of releasable silver species, or microbial recolonization after initial suppression. In contrast, samples modified with AgNPs by dip-coating did not exhibit visible inhibition zones at 24 and 48 h and showed signs of microbial contamination after 72 h (Figure 10d–f). The absence of detectable inhibition in dip-coated samples is consistent with the lower surface loading and retention of AgNPs expected from immersion-based coating, as supported by AFM observations. The contamination observed in the Kraft paper samples could be related to several factors: (1) inadequate sterilization, considering

that only one side of the paper discs was exposed to ultraviolet radiation; (2) possible cross-contamination from materials handled during the assay setup, such as forceps and pipette tips, which had been shared with other experiments; and (3) intrinsic characteristics of Kraft paper, particularly its high moisture retention capacity, which favors fungal growth. These issues highlight the need for improved sterilization strategies (e.g., autoclaving, plasma, and ethanol), controlled handling procedures, and possibly drying steps prior to plating to reduce moisture-associated contamination.

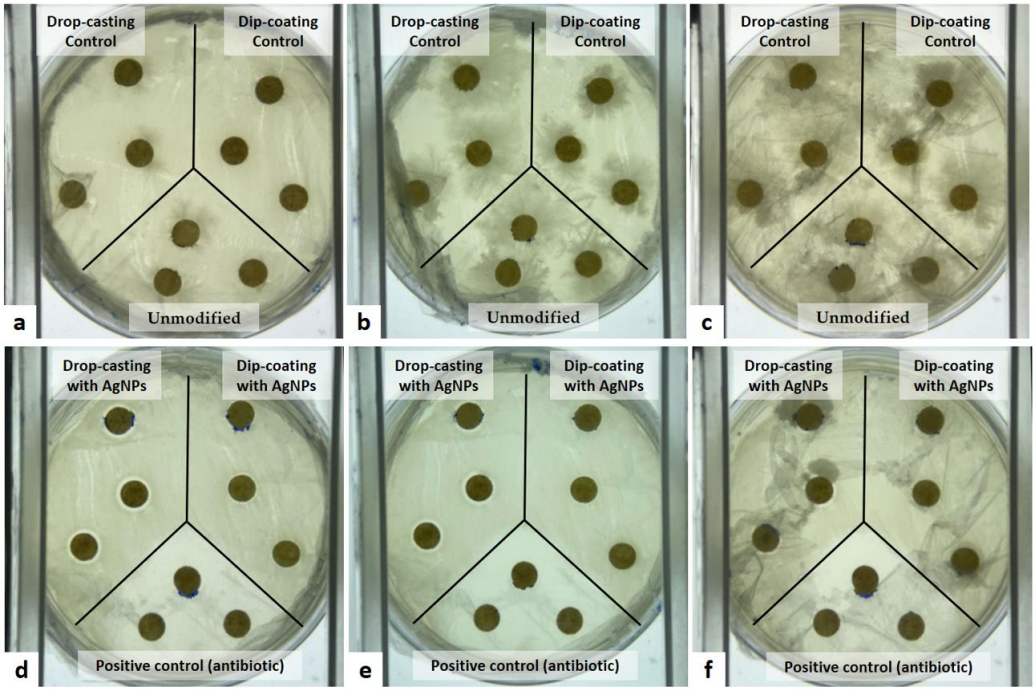

Figure 10. In vitro antibacterial activity assays of Kraft paper samples evaluated by disk diffusion test. (**a**–**c**) Unmodified Kraft paper and samples treated with distilled water by dip-coating and drop-casting, after 24, 48, and 72 h; (**d**–**f**) Kraft paper with antibiotic (positive control) and samples modified with AgNPs by dip-coating and drop-casting, after 24, 48, and 72 h.

The measurement of inhibition zones was performed using images obtained after 24 h of incubation and processed with ImageJ software (version 1.53m). The positive control (antibiotic-treated discs) exhibited a clear inhibition zone (21.37 $\pm$ 0.96 mm), confirming the responsiveness of the assay. In contrast, AgNP-modified samples exhibited substantially smaller inhibition zones, measuring 9.25 $\pm$ 0.13 mm for drop-casting and 7.92 $\pm$ 0.15 mm for dip-coating. While these zones suggest antibacterial activity, the measurements should be interpreted with caution due to concurrent microbial contamination, which likely interfered with accurate inhibition zone delineation. Moreover, the inhibition zones were substantially smaller than those observed for the antibiotic control, indicating that nanoparticle loading and surface retention may influence antimicrobial response, though insufficient to ensure sustained or robust activity under the present experimental conditions.

The antimicrobial performance observed in the present study contrasts with reports of strong antibacterial activity in other AgNP-cellulose systems. For instance, cellulose paper coated with silver-enhanced gold nanoparticles (Au–Ag NPs) and immobilized by heat treatment has shown sustained and effective inhibition of *E. coli* [29]. In comparison, the AgNP-modified Kraft paper evaluated here exhibited only limited and, in the case of drop-cast samples, transient inhibition, while dip-coated samples showed no measurable antibacterial effect. These differences suggest that physically deposited AgNP layers may provide insufficient silver availability or stability compared to chemically

or thermally immobilized coatings. Consequently, the antimicrobial efficacy of AgNP–cellulose materials is strongly dependent on the synthesis route, immobilization strategy, and nanoparticle distribution.

The drop-casting method resulted in the highest AgNP surface loading, consistent with the measurable inhibition zones observed at 24 and 48 h. However, this higher nanoparticle deposition was accompanied by pronounced surface heterogeneity and local agglomeration, which acted as microstructural stress concentration sites and reduced the maximum load, as indicated by force spectroscopy measurements. In contrast, dip-coating yielded lower AgNP retention and negligible antimicrobial activity but preserved mechanical integrity, suggesting more uniform nanoparticle–fiber interactions. These results highlight a central trade-off in the design of nanoparticle-functionalized paper: achieving higher antimicrobial efficacy may compromise structural performance, whereas mechanically safer coatings may provide limited antimicrobial protection. Optimizing deposition parameters or employing immobilization strategies could help balance these competing outcomes in future applications.

Based on the combined physicochemical, nanomechanical, and antimicrobial results, the AgNP-modified Kraft paper developed in this study is particularly suited for application scenarios where surface antimicrobial functionality is required without prolonged mechanical loading. Specifically, drop-cast AgNP coatings, which provided higher nanoparticle surface density and transient antibacterial activity, may be applicable in short-term food contact materials or secondary packaging components intended to reduce surface microbial contamination during handling, transport, or early storage stages [30]. Conversely, dip-coated samples, which preserved mechanical integrity but exhibited limited antibacterial activity, may be more appropriate for applications where structural performance is prioritized and antimicrobial action is not critical. These findings highlight the importance of selecting deposition strategies according to the intended packaging function, rather than seeking a single universally optimal coating approach.

4. Conclusions

The collective results obtained from physicochemical, nanomechanical, and antimicrobial activity analyses confirmed that the different modification techniques applied to Kraft paper samples with AgNPs imparted distinct alterations on the material's surface. AFM images revealed that samples treated by drop-casting exhibited structures consistent with nanoparticles adhered to the surface, unlike those modified by dip-coating. This outcome is attributed to the larger volume of suspension deposited using the drop-casting technique, resulting in a higher surface concentration of AgNPs on the substrate, but also in greater surface heterogeneity. These observations reinforce that deposition volume and solvent evaporation dynamics strongly influence nanoparticle retention and spatial distribution.

Furthermore, machine learning analysis using the Teachable Machine tool indicated lower confidence levels in classifying samples treated by drop-casting, suggesting that these surfaces exhibited greater morphological variability. The confusion matrix corroborated these results, showing increased misclassification among drop-cast groups due to uneven nanoparticle redistribution during solvent evaporation.

The incorporation of AgNPs via drop-casting led to a significant reduction in maximum load and adhesion force, indicating compromised mechanical strength and alterations in surface adhesiveness. These mechanical changes likely result from nanoparticle-induced microdisruptions in the fiber network, creating stress concentrators that weaken local structural integrity. Conversely, dip-coated samples retained comparatively higher stiffness, likely due to thinner and more uniform coating layers, but exhibited lower nanoparticle retention and minimal antibacterial effect.

In conclusion, drop-casting allows higher AgNP surface loading and transient antimicrobial activity, whereas dip-coating preserves mechanical integrity but delivers lower nanoparticle density and negligible antibacterial effect. These findings highlight a trade-off between functional performance and material strength. Future studies should focus on systematically optimizing drop-casting parameters such as nanoparticle concentration, applied volume, and drying conditions, to achieve a more uniform nanoparticle distribution while minimizing mechanical detriment. Additionally, studies could quantify AgNP migration under simulated food storage conditions, evaluate long-term antimicrobial performance, and assess the impact of coating thickness and substrate pre-treatment on both mechanical integrity and functional efficacy.

Author Contributions: Conceptualization, methodology, formal analysis, investigation, data curation, writing—original draft preparation, N.M.A.d.S.; Supervision, writing—review and editing, J.J.P.; Supervision, writing—review and editing, C.C.B.; Resources, supervision, project administration, writing—review and editing, funding acquisition, L.P.S. All authors have read and agreed to the published version of the manuscript.

Funding: This research was funded in part by the Coordenação de Aperfeiçoamento de Pessoal de Nível Superior—Brazil (CAPES—Finance Code 001 and no. 23038.019088/2009-58), Conselho Nacional de Desenvolvimento Científico e Tecnológico (CNPq no. 311825/2021-4, 307853/2018-7, 408857/2016-1, 306413/2014-0, and 563802/2010-3), Fundação de Apoio à Pesquisa do Distrito Federal (FAPDF no. 193.000.445/2008 and 193.000.429/2008), and Empresa Brasileira de Pesquisa Agropecuária (Embrapa no. 10.20.03.009.00.00, 23.17.00.069.00.02, 13.17.00.037.00.00, 21.14.03.001.03.05, 13.14.03.010.00.02, 12.16.04.010.00.06, 22.16.05.016.00.04, 11.13.06.001.06.03, and 10.19.03.054.00).

Institutional Review Board Statement: Authorization for access to the genetic patrimony (CGEN no. 02001.007580/2014-95). No additional ethical approval was required for this study, as it did not involve human or animal subjects.

Informed Consent Statement: Not applicable.

Data Availability Statement: The original contributions presented in the study are included in the article. Further inquiries can be directed to the corresponding author.

Acknowledgments: The authors wish to acknowledge the Postgraduate Program in Nanoscience and Nanobiotechnology, University of Brasília (UnB), Brasília, DF, Brazil, for providing academic support.

Conflicts of Interest: The authors declare no conflicts of interest. The funders had no role in the design of the study, analysis of data, or decision to publish this manuscript.

Abbreviations

The following abbreviations are used in this manuscript:

AFM	Atomic force microscopy
AgNPs	Silver nanoparticles
CFU	Colony-forming unit
DLS	Dynamic light scattering
HD	Hydrodynamic diameter
OD	Optical density
Pa	Pascal
PdI	Polydispersity index
Ra	Average roughness
ZP	Zeta potential

References

1. Silveira, D.J.; Durigan, A.; Monteiro, T.; Sgarbiero, I.M.; Silva, D.A. Influence of storage time and log length on the distribution of wood chip size. *BioResources* **2023**, *18*, 4510–4518. [CrossRef]
2. Gharehkhani, S.; Sadeghinezhad, E.; Kazi, S.N.; Yarmand, H.; Badarudin, A.; Safaei, M.R.; Zubir, M.N.M. Basic effects of pulp refining on fiber properties—A review. *Carbohydr. Polym.* **2015**, *115*, 785–803. [CrossRef] [PubMed]
3. Saad, A.S. Study of Kraft Paper Quality as a Function of Recycled Fiber Variation. Master's Thesis, São Paulo State University, Itapeva, Brazil, 2018; 74p. (In Portuguese)
4. Deshwal, G.K.; Panjagari, N.R.; Alam, T. An overview of paper and paper based food packaging materials: Health safety and environmental concerns. *J. Food Sci. Technol.* **2019**, *56*, 4391–4403. [CrossRef] [PubMed]
5. Bahmid, N.A.; Suloi, A.N.F.; Engelen, A.; Anwar, M.; Hernawan. Antimicrobial food packaging—Interaction of compounds and bacterial growth. *Curr. Food Sci. Technol. Rep.* **2024**, *2*, 121–131. [CrossRef]
6. Bumbudsanpharoke, N.; Ko, S. Nano-food packaging: An overview of market, migration research, and safety regulations. *J. Food Sci.* **2015**, *80*, R910–R923. [CrossRef]
7. Amini, E.; Azadfallah, M.; Layeghi, M.; Talaei-Hassanloui, R. Silver-nanoparticle-impregnated cellulose nanofiber coating for packaging paper. *Cellulose* **2016**, *23*, 557–570. [CrossRef]
8. Becaro, A.A.; Oliveira, L.P.; Castro, V.L.S.; Siqueira, M.C.; Brandão, H.M.; Correa, D.S.; Ferreira, M.D. Effects of silver nanoparticles prenatal exposure to rat offspring development. *Environ. Toxicol. Pharmacol.* **2021**, *81*, 103546. [CrossRef]
9. Tang, X.; Yan, X. Dip-coating for fibrous materials: Mechanism, methods and applications. *J. Sol-Gel Sci. Technol.* **2017**, *81*, 378–404. [CrossRef]
10. Venkatesan, K.K.; Samikannu, S. A two-dimensional nanomaterial-based fiber optic sensor for humidity and gas sensing application: In-depth review. *Phys. Scr.* **2024**, *99*, 062005. [CrossRef]
11. Bonatto, C.C. Development and Evaluation of In Vitro and In Vivo Biological Activities of Micro- and Silver Nanoparticles Obtained by Green Synthesis Using Cerrado Plants. Doctoral Dissertation, University of Brasília, Brasília, Brazil, 2016; 227p. (In Portuguese)
12. Silva, A.S.S.; Santos, J.H.Z. Sol-gel method for polymers. In *Nanotechnology Applied to Polymers*; Blucher: São Paulo, Brazil, 2022; pp. 459–496. [CrossRef]
13. Terra, I.A.A.; Aoki, P.H.B.; Delezuk, J.A.M.; Martins, M.A.; Manrich, A.; Silva, M.J.; Costa, M.M.; Torres, B.B.M.; Waldir, A., Jr.; Ferreira, C.S.G.; et al. Polymer characterization techniques. In *Nanotechnology Applied to Polymers*; Blucher: São Paulo, Brazil, 2022; pp. 497–590. [CrossRef]
14. Noronha, T.H.; Vieira, D.G.; Andrade, E.G.S.; Santos, W.L. Indicator of food fecal contamination and disease prevention. *Rev. JRG Estud. Acad.* **2019**, *2*, 150–157. (In Portuguese)
15. Oliveira, L.S.; Furtado, L.L.; Diniz, F.A.S.; Mendes, B.L.; Araújo, T.R.; Silva, L.P.; Santiago, T.R. Eco-friendly silver nanoparticles synthesized from a soybean by-product with nematicidal efficacy against *Pratylenchus brachyurus*. *Nanomaterials* **2024**, *14*, 101. [CrossRef] [PubMed]
16. Pupe, J.M.; Silva, L.P. Modulation of physico-chemical and biological properties of silver nanoparticles synthesized using aqueous extract of flamboyant (*Delonix regia* var. *flavida*, Fabaceae) seeds. *J. Clust. Sci.* **2021**, *32*, 1053–1060. [CrossRef]
17. Lin, S.; Wiesner, M.R. Deposition of aggregated nanoparticles: A theoretical and experimental study on the effect of aggregation state on the affinity between nanoparticles and a collector surface. *Environ. Sci. Technol.* **2012**, *46*, 13270–13277. [CrossRef] [PubMed]
18. Raheem, S.A.; Alfatlawi, A.H. Surface-water purification using cellulose paper impregnated with silver nanoparticles. *Drink. Water Eng. Sci.* **2021**, *14*, 95–102. [CrossRef]
19. Trotta, F.; Da Silva, S.; Massironi, A.; Mirpoor, S.F.; Lignou, S.; Ghawi, S.K.; Charalampopoulos, D. Advancing food preservation: Sustainable Green-AgNPs bionanocomposites in paper-starch flexible packaging for prolonged shelf life. *Polymers* **2024**, *16*, 941. [CrossRef]
20. Pavinatto, A.; Soares, A.C.; Torres, B.B.M. Drop-casting and dip-coating films. In *Nanotechnology Applied to Polymers*; Blucher: São Paulo, Brazil, 2022; pp. 303–326. [CrossRef]
21. Canevarolo, S.V., Jr. *Polymer Science: A Basic Text for Technologists and Engineers*; Artliber Editora: São Paulo, Brazil, 2002. (In Portuguese)
22. Lähdetie, A.; Nousiainen, P.; Sipilä, J.; Tamminen, T.; Jääskeläinen, A. Laser-induced fluorescence (LIF) of lignin and lignin model compounds in Raman spectroscopy. *Holzforschung* **2013**, *67*, 531–538. [CrossRef]
23. Agarwal, U.P. Analysis of cellulose and lignocellulose materials by Raman spectroscopy: A review of the current status. *Molecules* **2019**, *24*, 1659. [CrossRef]
24. Braga, P.C.; Ricci, D. (Eds.) *Atomic Force Microscopy: Biomedical Methods and Applications*; Methods in Molecular Biology; Humana Press: Totowa, NJ, USA, 2004; Volume 242.
25. Bhushan, B.; Harald, F.; Kawata, S. *Applied Scanning Probe Methods V*; Springer: Berlin/Heidelberg, Germany, 2006. [CrossRef]

26. He, Y.; Li, H.; Fei, X.; Peng, L. Carboxymethyl cellulose/cellulose nanocrystals immobilized silver nanoparticles as an effective coating to improve barrier and antibacterial properties of paper for food packaging applications. *Carbohydr Polym.* **2021**, *252*, 117156. [CrossRef]
27. Rhim, J.-W.; Park, H.-M.; Ha, C.-S. Bio-nanocomposites for food packaging applications. *Prog. Polym. Sci.* **2013**, *38*, 1629–1652. [CrossRef]
28. Pinto, T.J.A.; Kaneko, T.M.; Ohara, M.T. *Biological Quality Control of Pharmaceutical, Related Products and Cosmetics*, 2nd ed.; Atheneu Editora: São Paulo, Brazil, 2003. (In Portuguese)
29. Tsai, T.T.; Huang, T.H.; Chang, C.J.; Ho, N.Y.J.; Tseng, Y.T.; Chen, C.F. Antibacterial cellulose paper made with silver-coated gold nanoparticles. *Sci. Rep.* **2017**, *7*, 3155. [CrossRef]
30. Srikhao, N.; Ounkaew, A.; Srichiangsa, N.; Phanthanawiboon, S.; Boonmars, T.; Artchayasawat, A.; Theerakulpisut, S.; Okhawilai, M.; Kasemsiri, P. Green-synthesized silver nanoparticle coating on paper for antibacterial and antiviral applications. *Polym. Bull.* **2023**, *80*, 9651–9668. [CrossRef]